ARTICLE NO. 79-0922R

A80-081

Electrostatically Formed Antennas

30018
70030
80004

Dennis J. Mihora* and Peter J. Redmond†
General Research Corporation, Santa Barbara, Calif.

Large lightweight reflector antennas in Earth orbit are the key to realizing many applications of infrared and radiometric sensors. Many of these applications call for reflector diameters of 10-200 m and rms surface qualities of 0.1-1000 μm. A concept for achieving such a high surface quality in a reflector that is inherently lightweight and compact has been studied over the last few years. The concept is that of using electrostatic forces to tension a thin conducting membrane and maintain it in a precision antenna shape. This electrostatically controlled membrane mirror is an adaptive structure that maintains surface quality despite errors in construction, irregularities of materials, solar heating, and on-board disturbances.

Nomenclature

A = area of plate or aperture area
d = unperturbed central deflection
E = Young's modulus of elasticity or electric field strength
f_S = spring restoring force
f_N = ratio of focal length to aperture diameter
g = generalized function
G = structural damping factor as a fraction of the critical damping coefficient
G_{dB} = electromagnetic gain ratioed to isotropic
l = effective membrane-electrode spacing or characteristic width of shell
m = mass of plate
n = integer index on the radial spatial wavenumber
p = pressure
r = radial coordinate
R = radius of aperture at perimeter
t = membrane or shell thickness
U = potential function
V = voltage
y = membrane-electrode separation
Δ_n = surface error/fractional pressure error
ΔR = increment of rim out-of-roundness
Δz = central membrane deflection
ΔZ = half-amplitude rim out-of-flatness
ϵ = material strain
ϵ_0 = 8.85×10^{-12} F/m, free space dielectric constant
λ = wavelength of electromagnetic energy
ρ = material density or radius of curvature
ν = fractional pressure error
θ = angular rotation of membrane element
σ = material stress
σ_y = 6.89×10^7 N/m^2, assumed polymer yield stress
ω = natural frequency

Subscripts

b = secondary equilibrium point
c = critical condition
e = equilibrium point
0 = initial condition
r = radial direction
y = yield condition
θ = azimuthal direction

Presented as Paper 79-0922 at the AIAA/NASA Conference on Advanced Technology for Future Space Systems, Hampton, Va., May 8-11, 1979; submitted June 18, 1979; revision received Jan. 24, 1980.

Index categories: Structural Design; Spacecraft Systems; Satellite Communication Systems.
*Member of Technical Staff, Aerospace Sciences Division. Member AIAA.
†Member of Technical Staff, Aerospace Sciences Division.

Introduction

THE electrostatically controlled membrane mirror[1] (ECMM) is a revolutionary approach to achieving large, very light reflectors for radar, radio astronomy, radiometry, and optical devices. The ECMM is a thin electrically conducting membrane that is accurately tensioned and positioned by electrostatic (Coulomb) forces. The reflector's shape (figure) is maintained by varying the electrical potential between the membrane and segmented electrodes behind it, using closed-loop control. An important component of this adaptive structure is the figure sensor, that monitors the surface quality to furnish error signals to the control loop.

Analytical and experimental efforts in the last several years indicate the possibility of employing the ECMM for high-surface-precision reflectors in both ground and space applications. In both situations, design goals are to achieve a ratio of aperture diameter to rms surface waviness of 10^5-10^9. Achieving such precision in light structures is difficult, if not impossible, without some form of active control. With active control—positioning the membrane to a required figure automatically—surface precision may be achieved despite the presence of various disturbances. In effect, great improvements in surface accuracy over passive reflectors are expected because optical-electrical circuitry can provide long-term positional stability of the membrane.

The ECMM was initially conceived as the outcome of studies to define new approaches to achieving very lightweight reflectors that would utilize the materials and the control technology that have unfolded over the last decade. It was noted that the reflection of electromagnetic energy requires a surface only a few hundred angstroms for optical and millimeter waves. Conventional reflectors, however, require deep supporting structures to achieve stiffness; the reflecting surface itself weighs an insignificant fraction of the support structure's weight. An obvious direction for reducing the reflector's mass is to reduce its thickness until it becomes a membrane, and stiffen it by some means other than the material's flexure resistance. Figure 1 illustrates the two techniques for achieving stiffness (that is, raising vibrational frequency). An isotropic shell has a lowest-mode frequency proportional to $\sqrt{E/\rho t/l^2}$. A stressed membrane has a frequency proportional to $\sqrt{E/\rho g(\epsilon,\theta)}/l$. The membrane achieves its stiffness through the extensional and geometrical terms ϵ and θ rather than the mass-dependent thickness term (t/l) of the shell structure. The stressed membrane also provides a dramatic benefit of achieving a very smooth surface, which will be discussed later.

Analysis and design of the ECMM have been pursued over the last four years. Small-scale experiments have shown that optical-quality surfaces can be achieved, using membranes controlled and tensioned by electrostatic forces. Experiments were performed in the early 1960's[2] using colloidal membranes. More recently, several experimenters have utilized custom high-precision membranes of Mylar‡ and Parylene§ to approach infrared surface quality. Both pneumatic and electrostatic forming of membranes to millimeter-wave surface quality have been accomplished on 1 m apertures. In recent months, the ECMM studies have focused on a 4.88 m ground-based model that is currently being tested. Also, recent configuration design studies have led to a 95 GHz, 90 dB gain radiometer configuration that is 30 m in diameter but can be stored in 1/5 of the Space Shuttle's bay. This paper will describe these advanced-technology concepts.

The ECMM Concept

The ECMM, shown schematically in Fig. 2, is essentially a charged capacitor with the deformable reflector as one of its electrodes. When a voltage is applied between the unstressed membrane (dashed line) and the back electrodes (distributed control segments), the electrostatic attractive force draws the membrane inward. An electrical network is used to generate the required high field strength between the supported back electrodes and the deformable membrane electrode. The pressurized membrane deforms to a doubly curved surface, unlike "draped-mesh" reflectors, that are made up of flat or singly curved sections. A membrane acted upon by a pressure loading naturally forms a concave surface of the sort required for most antenna reflectors. The fixed back control electrode is segmented into electrically isolated elements, each supplied with a different control voltage and thus exerting a different field strength and pressure on the membrane. Like pneumatic pressure applied to a deformed balloon, the electrostatic force is always normal to the (conducting) membrane; but unlike pneumatic pressure, the electrostatic loading can be rapidly changed and can be different at different points on the membrane, thus forming different reflector geometries.

Each electrode has a relatively wide influence region extending beyond its perimeter, so that the electrodes impart a smoothly varying pressure distribution to the membrane. This is a strong distinction between the ECMM and the mechanically actuated segmented-shell reflectors. The expectation of achieving reflectors accurate enough for optical wavelengths resides in the very favorable form of the loading imparted to the membrane by the control electrodes and in the unique response of a nonlinear membrane that has undergone large deflections (and angular rotations) while experiencing small strains. This combined response of electrostatics and the membrane has resulted in ECMM configurations that appear to require a very low number of control servos (electrodes).

To achieve and control the membrane tension requires a spatially and temporally controllable pressure field on the membrane. Electrostatic pressures appear the most usable because 1) they are readily controllable, 2) they can be an integral part of the electro-optical control system, 3) they can provide enough pressure to contour membranes of a thickness that can be reasonably handled and manufactured, and 4) they can be maintained with insignificant power or current flow.

Adaptive control of the tensioned membrane employs classical closed-loop servo techniques in conjunction with recent developments in optical (inteferometric) figure sensing to provide the position information. As the membrane deviates from its required position, the figure sensor generates an error signal that a processor then translates into voltage change, resulting in a pressure correction. Delays in the loop can be very short, since the loop is entirely electrical. Voltage changes at the back electrodes result in nearly instantaneous changes in the pressure loading on the membrane.

‡Trademark of Dupont.
§Trademark of Union Carbide.

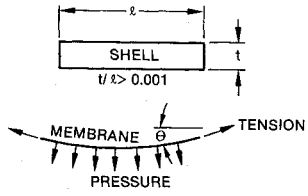

Fig. 1 Mechanisms for achieving stiffness.

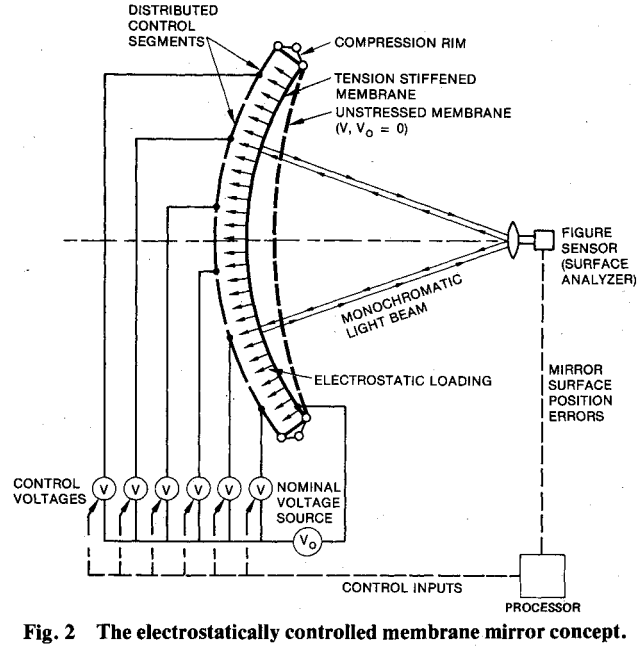

Fig. 2 The electrostatically controlled membrane mirror concept.

High-Payoff Applications

One figure of merit for an antenna reflector is the ratio of its diameter to surface accuracy D/σ. The electromagnetic gain of the radiating reflector compared to a radiating dipole, and the imaging ability of the reflector, are directly related to D/σ. In general, σ must be a small fraction of the electromagnetic wavelength λ. The ECMM is expected to introduce significant performance improvements over passive reflectors, which have severe limits on D/σ if they are to be reasonably light. The relationships between frequency, size, and the antenna gain is $G_{dB} = 10 \log (4\pi A/\lambda^2)$. The surface smoothness is specified to be $\lambda/50$, a value that virtually eliminates any effect of surface roughness on gain. Design concepts in the current literature emphasize the 1-12 GHz frequency band (S,C,X) which for high-performance (80-100 dB gain) missions, would necessitate extremely large space structure. Several "windows" at higher frequencies, e.g., 30, 95, and 245 GHz, are being evaluated for radiometers because of the reduction in aperture size for the same gain. The significance of operating at the higher frequency windows is shown in Table 1 which compares the size of the apertures to obtain the same one-way gain of 90 dB (including transmission through the atmosphere). Figure 3 indicates the

Table 1 Operating frequency vs aperture size

Frequency, GHz	Diameter, m
2	1425
8	356
95	38

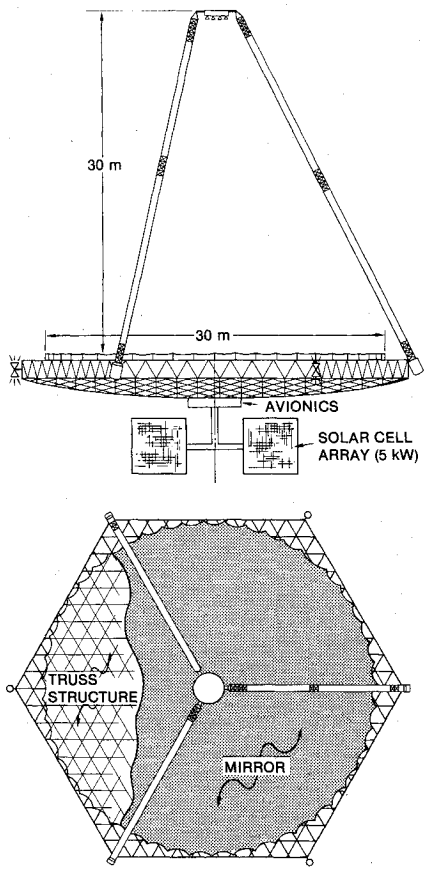

Fig. 3 Fully deployed 30 m radiometer with ECMM, gain = 90 dB at 95 GHz.

layout of a satellite with a 90-dB-gain antenna that could be packed into 1/5 of the Shuttle's bay. Packaging studies[3] indicate the possibility of obtaining 100 dB gain from a large aperture that could be stored in ½ of the Space Shuttle's bay.

Although the highest payoff for the ECMM appears to be at the millimeter wavelengths, designs at centimeter wavelengths (S,C,X bands) are being pursued because the layouts are much simpler than the millimeter-wave configuration shown in Fig. 4.

The ECMM appears promising for several additional applications. First, high-gain ground-based reflectors can operate without electrical breakdown in air. Gravity-induced deformations of the extremely light membrane are insignificant. Gravity sag of a very low mass electrode support structure is compensated by controlling the voltage between the membrane and the control electrodes. Secondly, a high-gain high-resolution radio telescope in orbit[4] operating at 600-1000 GHz with a diameter of 30 m is discussed as the next important step in astronomy.

Studies[5,6] have also proceeded to address the first-order technical issues of large millimeter-wave or infrared optical reflectors. These, however, would require the manufacturing of large precision membranes. One candidate is Parylene, which can be vacuum polimerized onto an optical glass surface and then removed. Quality control specifications for the membrane used in infrared reflectors are very demanding but appear achievable with current technology.

ECMM Subscale Models

The concept of the large deformation of a thin membrane into a curved reflecting surface by using electrostatic forces first appeared in a 1932 British patent by Muller.[7] A refinement of this concept into an elementary reflector was patented in 1967 by H.S. Jones.[8] Using principally colloidal membranes, Jones achieved infrared optical quality on small

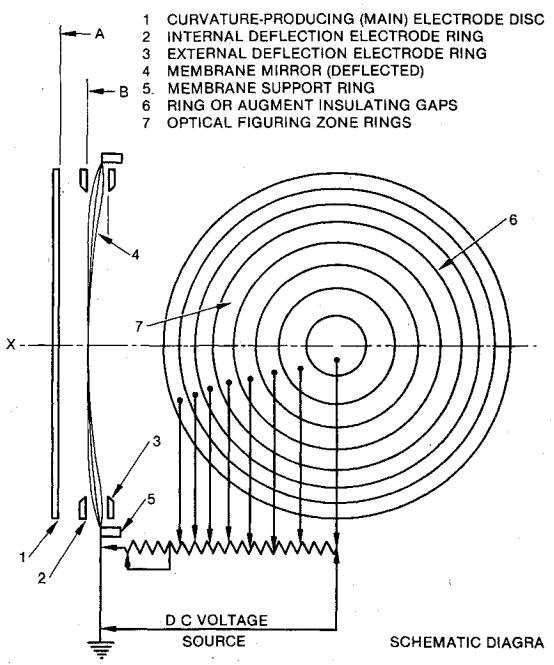

Fig. 4 Membrane mirror with electrically rotatable optical axis.

models (10-20 cm) with one control electrode. Figure 4 indicates one of Jones' schematic layouts of an optical membrane mirror.

Because of the extremely light mass and excellent dynamic controllability, electrostatically controlled membranes are also used as audio transducers in high-fidelity speakers and earphones. Several of the commerical electrostatic speaker systems incorporate controlled membranes 1 to 1.5 m across.

Various tests on small scale (1 to 2 m diam) reflectors (see Fig. 5) have recently been completed[5] in which both pneumatics and electrostatics were applied to commerical membranes. In the pneumatic tests, the measured reflector shape agreed with theory to 30 μm which was the accuracy of the particular optical measuring equipment. Electrostatic models have investigated the electrical-mechanical (position) stability of the membrane as a function of applied voltage. Finally, several types of rim "catenaries" allow perimeter attachment at a few discrete stations rather than continuously along the perimeter. A simple catenary attachment provides for many options of deploying and supporting the membranes in space.

Testing of a 4.88 m configuration is tentatively planned for 1980. Figure 6 is a scale drawing of this spherical aperture, which is formed from a flat sheet of Kapton 7 μm thick. The purposes of the experiment include the following.

Electrostatic shaping using at least five concentric electrodes will demonstrate the active control of a structure to form various reflector geometries and focal lengths. The model will demonstrate the smoothing and improvement in surface quality by application of electrostatic pressure. Principally, this model test will provide a materials evaluation with large sampling areas of commerical polymer membranes. Data will be obtained on membrane homogeneity, isotropy, thickness variability, and waviness. The effects of seams in the reflector will also be observed.

The deflection of membrane at its center upon application of the voltage from the 4.88 m spherical aperture will be 8.71 cm. The membrane-electrode gap is three-quarters of the membrane deflection. The pressure required to deform the membrane is approximately 1.9 N/m^2, which is achieved by applying a voltage of 43 kV at the center or an electric field intensity of 660 kV/m. The electrostatic pressure is small by one comparison, being about 2×10^{-5} times solar pressure. Although the voltages are high, the current flow and energy

Fig. 5 ECMM model (1.0 m) incorporating commercial membranes and a single electrode: (left) Kapton membrane with catenary and spring perimeter, (center) Mylar membrane untensioned, (right) same Mylar membrane with electrostatic forces.

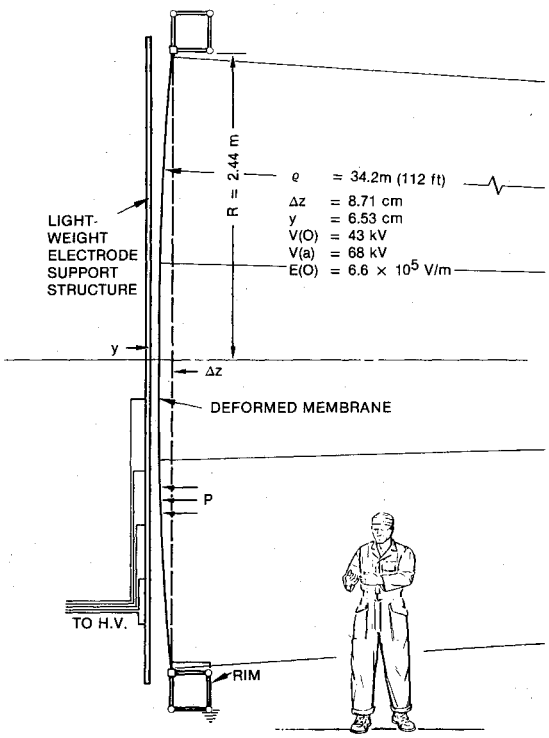

Fig. 6 Proposed spherical ECMM, $f_N = 3.5$.

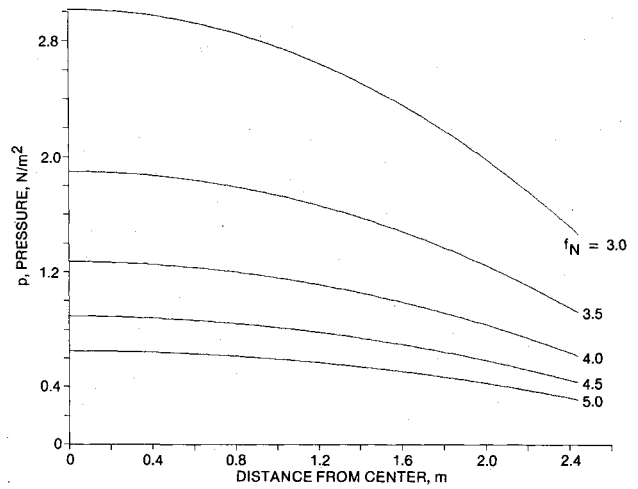

Fig. 7 Pressure loading required to form spherical reflectors from flat membrane.

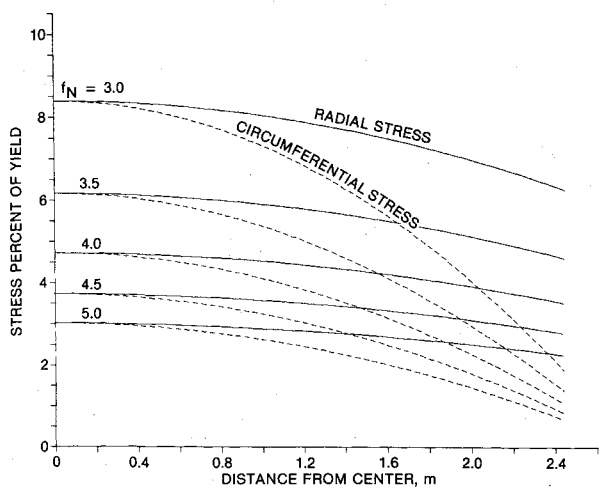

Fig. 8 Radial and circumferential stresses in spherical reflectors formed from flat membrane.

storage are very small. The 4.88 m model acting as a storage capacitor contains only about 0.4 J of electrical energy which is a consequence of the small capacitance of about 4.4×10^{-9} F.

The remainder of this paper will discuss some of the characteristics of the ECMM determined from recent studies.

ECMM Characteristics

Static Shape Forming

The application of electrostatic pressure on a thin membrane can produce large deflections and rotations while incurring small strain. Linear Hookean material properties have been included in the analysis of many reflector geometries. An "inverse" numerical solution has been developed,[9] in which the unloaded and loaded membrane shapes are specified and the electrostatic loading and internal stresses are determined. A variety of ECMM characteristics will now be presented in which the initial, unstressed membrane shape is flat and the deformed shape is spherical. The membrane is rigidly attached to a continuous rim. Figure 7 indicates the pressure distribution as a function of radius for differnt f_N numbers. There is a characteristic dropoff of the pressure, the value at the perimeter being approximately one-half that at the center. Analyses[6] and tests have been performed on membranes with constant pressure loadings. The resulting shape is far from circular or parabolic, with about a factor of two difference in curvature between the center and the perimeter. Thus, spatial load variations are necessary.

The membrane stresses associated with the spherical reflector are shown in Fig. 8. Both radial and circumferential stress are shown as fractions of yield stress. The two stresses are identical at the center. The circumferential stress decreases much more rapidly than the radial stress as one approaches the perimeter. The ratio of the stresses at the perimeter is Poisson's ratio for the membrane. At an f_N of about 2.8 the

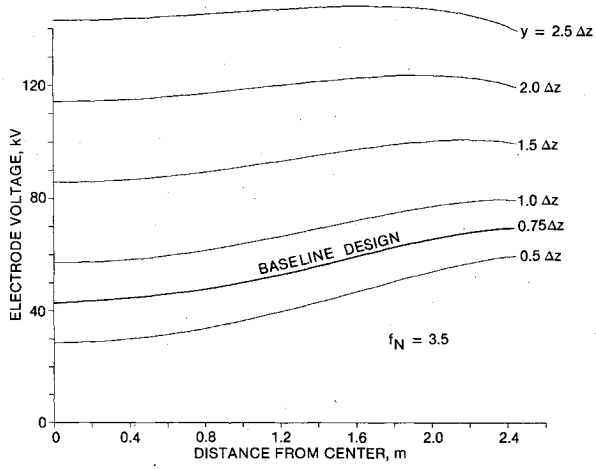

Fig. 9 Voltage distribution required to form spherical reflectors from flat membrane.

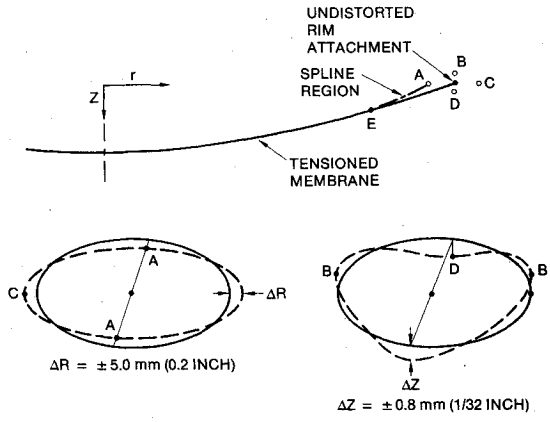

Fig. 10 Compensation for rim errors.

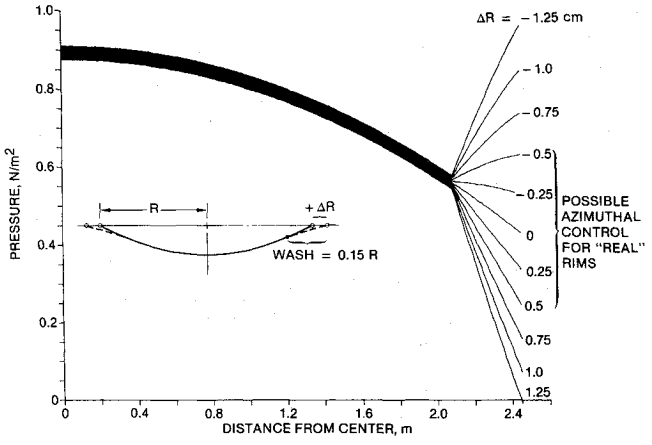

Fig. 11 Pressure corrections to compensate for rim errors, $f_N = 4.5$.

largest stress in the membrane is only one-tenth of yield. Although even lower f_N can be achieved with a flat sheet, this intermediate stress level is desirable, at this date, to minimize crack propagation and microcreep. For a lower f_N, the membrane can be preformed, probably to a spherical shape. From a preformed spherical membrane, the deformed shape can be other spheres and parabolas. The pressure distribution required to generate a parabola with $f_N = 1$ from various preformed spheres has been found to be similar to the previous cases.

Returning to the sphere formed from the planar sheet, the back control electrode voltage can be obtained from the required pressure distribution (Fig. 7) and the membrane-to-

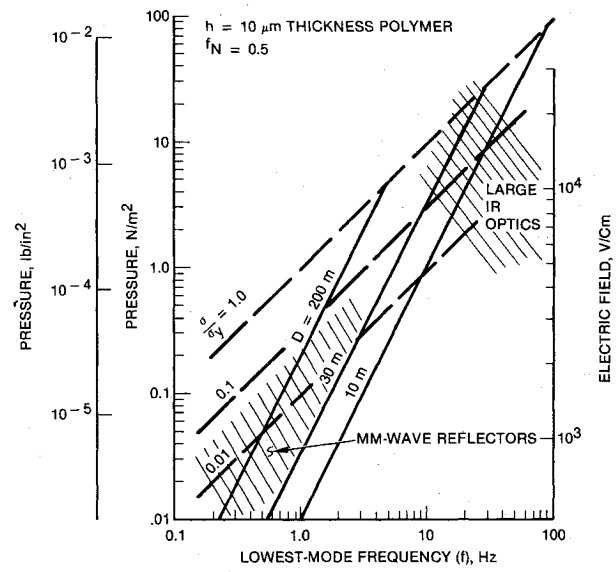

Fig. 12 Pressure requirements to achieve a specified vibrational frequency.

electrode spacing. The electrode voltage is approximately $V = y\sqrt{2p/\epsilon_0}$. There are many choices for the spacing y as a function of distance from the center. However, the spacing at the center must be at least a minimum value that satisfies the constraint discussed in the subsequent "stability" section. Two interesting back electrode geometries are a flat plate and a curved shape that permits constant voltage over the entire surface. The voltage as a function of distance from the center for the flat electrode is shown in Fig. 9 for $f_N = 3.5$ and various values of y. The gap y is presented as a function of the central membrane deflection Δz. Stability constraints require y of nearly $0.5\Delta z$. Large y such as $2.5\Delta z$ yield small radial voltage fluctuations but at the expense of large voltages. A nominal y of $0.75\Delta z$ has been selected for the 4.88 m model. Matching the voltage distribution with a finite number of electrodes will be discussed later.

Adaptive Forming

A particularly attractive aspect of the ECMM is its ability to accommodate large changes in the shape of portions of the membrane. Rather small membrane strains occur with large deflections. It is possible to alter the reflector's focal length and even its form, e.g., from axisymmetric to off-axis, the latter being possible with the introduction of azimuthal electrode segmentations. Azimuthal pressure control can provide significant reshaping of the membrane near a deformed attachment rim. The techniques to compensate for large rim errors of the types shown in Fig. 10 were examined for the 4.88 m model. The proposed solution, shown in Fig. 10, utilizes a splined region near the perimeter to "wash out" geometric errors.

Inboard of the splined region, the tensioned membrane is nearly axisymmetric. The large errors in the geometry of the rim can be constrained to the spline region. On the 4.88 m, $f_N = 4.5$ model, a 0.35 m spline can attenuate large rim distortions such as a rim out-of-roundness of $\Delta R = \pm 5$ mm (0.2 in.) and a rim out-of-flatness of $\Delta Z = \pm 0.8$ mm (1/32 in.).

Pressure corrections to ameliorate radial rim errors are shown in Fig. 11. For a positive radial displacement ΔR the electrostatic pressure must be reduced in the washout region. For a negative rim displacement, the electrostatic pressure must be increased. The limiting displacement for this example is a positive radial displacement $\Delta R = 1.25$ cm, because the pressure becomes zero at the rim. This electrostatic configuration cannot produce negative (repulsive) forces. Various geometric shapes can be selected for the washout region. In

this example, a polynomial up to cubic terms was selected. Therefore, the pressure corrections shown in Fig. 11 are not unique since other spline geometries can be postulated; however, these pressures are indicative of perimeter control requirements.

Stiffness

High levels of structural stiffness can be developed with thin membranes by the action of electrostatic forces causing large displacement and stress in the membrane. A high stiffness, or natural frequency, is an asset particularly if it can be obtained without a mass penalty. With membrane structures, higher frequency is obtained by increasing the pressure or stress in the membrane. Figure 12 summarizes the pressure and electric field associated with the lowest membrane frequency for an f_N of 0.5. Our nominal designs have a $\sigma/\sigma_y = 0.1$, which yields a frequency of about 9 Hz for a 30 m aperture. The electric field necessary to deform the membrane is quite important, since it is limited by breakdown effects. The breakdown electric field in a high vacuum is dependent principally on the materials and geometry of the electrodes and occurs in the range 5×10^4-10^6 V/cm. At atmospheric pressure, breakdown occurs between smooth electrodes at 3.2×10^4 V/cm. The onset of corona at 8×10^3 V/cm is usually selected as the limiting field strength. Requested frequencies for the ECMM have ranged from 1 to 50 Hz for 10 to 200 reflectors. In most of our designs, the natural frequency of the membrane reflector has been higher than that of the support structure. For most space-based applications, the 1 to 50 Hz lowest-mode frequency of the reflector is considerably higher than the on-board disturbances. The membrane's response to a low-frequency cyclic excitation is basically a static deflection response.

In an extremely demanding infrared optics application, the ECMM was excited at about 40 Hz, which was between modal eigenvalues of the membrane. The response of a 30 m ECMM to cyclic excitation is shown in Fig. 13. The transmissibility of the membrane is the ratio of the rms vibration (averaged over the whole surface) to a perimeter displacement. The response is presented for two membranes with damping $G=5\times10^{-4}$ and 10^{-2} (as fractions of critical damping). The resonant response of the ECMM is proportional to $1/G$. For this example, the aperture f_N was 0.5 and the membrane stress was about one-tenth of yield. The transmissibility at resonance of the tensioned membrane is actually small, considering the small values of damping that are postulated. In cases where rim vibrations have large amplitude, active control of the ECMM is proposed. Active control has been used to provide electrical "stiffening" and damping of specific membrane modes by proper design of the feedback control loop. The limitations on controllability is principally the frequency response of the figure sensor. The servo actuator (electrodes), sensor, and processor are all electrical and can therefore have a fast response. In situations where the rim vibrational displacements are small, the membrane response even at resonant frequencies may be tolerated. In most situations, the membrane's lowest-mode frequency is significantly higher than the excitations and the transmissibility is less than 1.0.

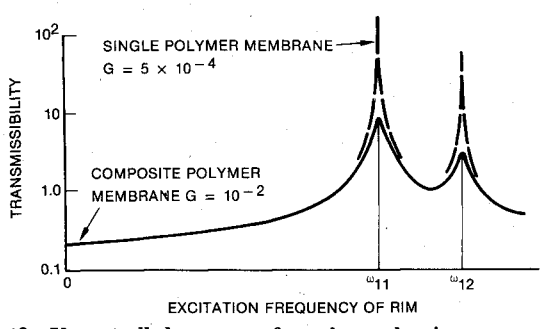

Fig. 13 Uncontrolled response of membrane showing resonances.

Stability

The deformation of an ECMM is established as a result of an equilibrium between electrical forces acting on and elastic forces acting in the surface. For a range of parameters such a system can be unstable. A membrane operating unstably typically accelerates towards the back electrode until the electric field exceeds breakdown. The membrane oscillates, repeatedly arcing, moving away from the electrode until the charge on the membrane is restored so that the membrane is again accelerated toward the electrodes.

Although it is conceivable that closed loop dynamic control would enable operation in an unstable regime it is far simpler to work at a stable equilibrium. Although detailed numerical calculations can be used to evaluate a given design for stability it is useful to consider simplified models in order to gain insight into the factors which influence stability.

Consider a parallel plate condensor (illustrated in Fig. 14) in which one of the plates is movable and held by a spring. If V is applied across the plates the electric field $E=V/z$ (neglecting end effects) exerts a force $\epsilon_0 A V^2/(2z^2)$. The acceleration of a plate is given by

$$m\ddot{z}=f_s(z)-\tfrac{1}{2}\epsilon_0 A V^2/z^2 \tag{1}$$

Any solution of

$$2z_e^2 f_s(z_e)=\epsilon_0 A V^2 \tag{2}$$

with $z_e>0$ corresponds to an equilibrium point at plate separation $z=z_e$. The frequency of small oscillations about such an equilibrium is determined by

$$-m\omega^2=\frac{\mathrm{d}f_s(z_e)}{\mathrm{d}z_e}+\frac{\epsilon_0 A V^2}{z^3} \tag{3}$$

and $\omega^2>0$, $\omega^2<0$, $\omega^2=0$ correspond, respectively, to stable, unstable, and neutral stability. At the boundary between stable and unstable operation ($\omega^2=0$) these equations imply

$$z_e\frac{\mathrm{d}f_s(z_e)}{\mathrm{d}z_e}=2f_s(z_e) \tag{4}$$

a result which depends only on the force function of the spring.

For generality nonlinear springs are considered with

$$f_s(z)=k_n(z-z_0)^n \tag{5}$$

and n is an odd integer. The solution of Eq. (4) indicates that the model system is stable if $(n+2)z_e>2z_0$. As the exponent n increases smaller plate separations are possible before going unstable. A membrane with a high pretension behaves linearly ($n=1$) while for an initially untensioned membrane the cube of the displacement is proportional to the applied pressure ($n=3$).

At the stable-unstable boundary there is a critical voltage V_c such that

$$(n+2)^{n+2}\epsilon_0 A V_c^2=8n^n k_n z_0^{n+2} \tag{6}$$

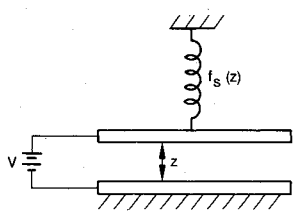

Fig. 14 Parallel plate capacitance model for stability analysis.

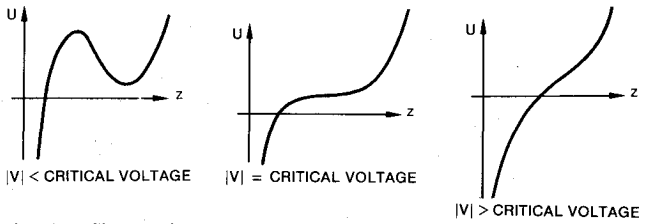

Fig. 15 Shape of potential energy curve as a function of applied voltage.

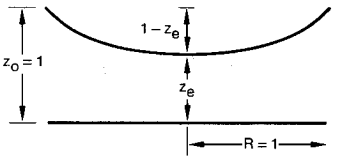

Fig. 16 Drumhead model for stability analysis.

For $|V| < |V_c|$ a stable equilibrium exists at a separation $(n+2)z_e > 2z_0$. There is an additional unstable equilibrium at a smaller separation $(n+2)z_e < 2z_b$. If the voltage is raised from zero to a value $|V| < |V_c|$ the plates will end in the vicinity of the stable equilibrium. In order to gain access to the unstable equilibrium it is necessary to raise the voltage to a value $|V| > |V_c|$ and then reduce $|V|$ to its final value with $|V| < |V_c|$.

For $|V| > |V_c|$ Eq. (2) has no positive solutions and no equilibrium exists. For all values of the separation z the force has the same sign—bringing the two plates together.

The net force on the plate is derivable from a potential function

$$U = k_n \frac{(z - z_0)^{n+1}}{n+1} - \frac{\epsilon_0 A V^2}{2z} \tag{7}$$

with a general shape shown in Fig. 15. The change in shape as the voltage varies provides a graphic illustration of the relations just described.

The one-degree-of-freedom parallel plate model provides a conservative estimate of the stable-unstable boundary. In a typical application only the central region of the membrane gets very close to the electrodes and the outer region provides a stabilizing influence. To show this effect, consider the next complicated model—the drumhead, a membrane sufficiently pretensioned so that the tensions do not appreciably change as the membrane is deformed. The geometry is illustrated in Fig. 16. The electric field is estimated by $E(r) \sim V(r)/y(r)$. With an appropriate choice of units the equation for the time variation of the deflections can be put in the dimensionless form

$$\ddot{y} = \frac{1}{r}\frac{\mathrm{d}}{\mathrm{d}r} r \frac{\mathrm{d}}{\mathrm{d}r} y - \frac{V^2}{y^2} \tag{8}$$

If the membrane is attached to a rigid rim at $r = 1$ suitable boundary conditions are $y(1) = 1$ and $\mathrm{d}/\mathrm{d}r\, y(r) = 0$ at $r = 0$. For small oscillations about the equilibrium position the frequency of oscillation is determined by the eigenvalue problem

$$-\omega^2 \delta y = \frac{1}{r}\frac{\mathrm{d}}{\mathrm{d}r} r \frac{\mathrm{d}}{\mathrm{d}r} \delta y + \frac{1}{2}\frac{V^2}{y^3}\delta y \tag{9}$$

with boundary conditions $\delta y(1) = 0$ and $(\mathrm{d}/\mathrm{d}r)\delta y = 0$ at $r = 0$. Given a static shape $y(r)$ the appropriate $V^2(r)$ to achieve this shape is given by

$$V^2(r) = y^2(r) \cdot \frac{1}{r}\frac{\mathrm{d}}{\mathrm{d}r} r \frac{\mathrm{d}}{\mathrm{d}r} y(r) \tag{10}$$

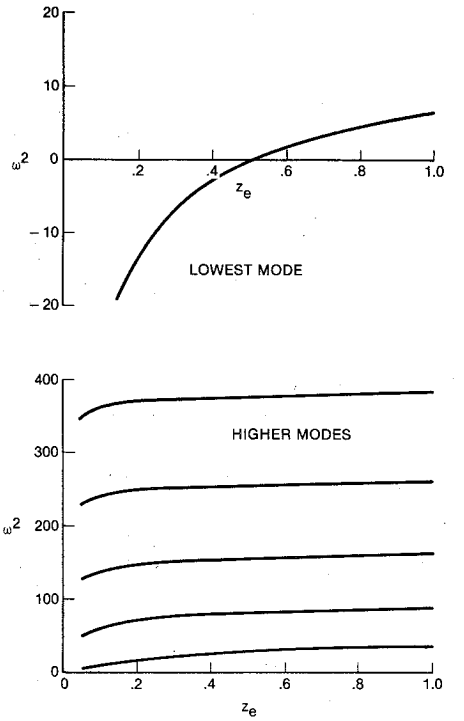

Fig. 17 Variation of ω^2 with separation.

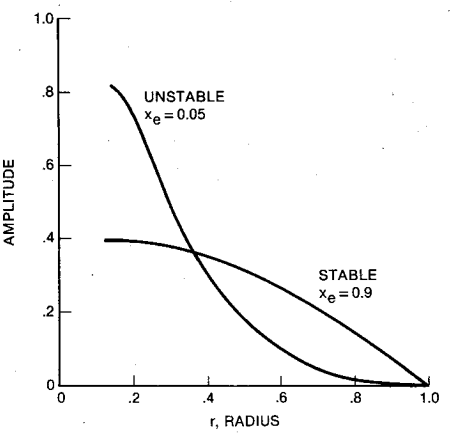

Fig. 18 Comparison of stable and unstable modes.

Conversely, for a given pressure profile (i.e., V^2/y^2 specified) it is possible to solve Eq. (8) with $\ddot{y} = 0$. The latter approach was adopted and for a constant pressure profile

$$y(r) = z_e + (1 - z_e) r^2 \qquad V^2/y^2 = 4(1 - z_e) \tag{11}$$

In the 4.88 m model the pressure profile is approximately quadratic, falling off to about half its central value, $V^2/y^2 = (1 - r^2/2)$, and solving Eq. (8) gives a profile

$$y(r) = z_e + (8/7)(1 - z_e)(r^2 - r^4/8) \tag{12a}$$

$$V^2/y = (32/7)(1 - z_e)(1 - r^2/2) \tag{12b}$$

It is interesting to note that although the two pressures given by Eqs. (11) and (12) are significantly different (as much as 50%), profiles with the same central deflection differ only slightly from each other (less than 4% of the central deflection everywhere).

The eigenvalue problem, Eq. (9), was solved numerically and the results are shown in Fig. 17. These results are for the nonuniform pressure variation Eq. (12). The results for uniform pressure are essentially the same.

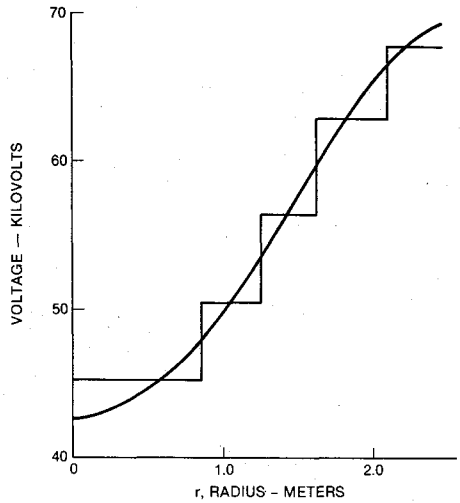

Fig. 19 Voltage profile for reflector.

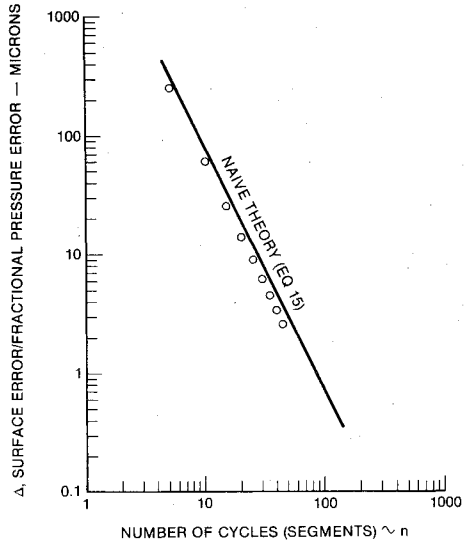

Fig. 20 Surface quality variation with number of electrodes, Δ_n.

The lowest mode goes unstable at $z_e = 0.5$ (compared to the linear one-degree-of-freedom value $z_e = 0.667$) while the higher modes remain stable even for very small electrode-membrane central separations.

The eigenfunctions, $\delta y(r)$, for the stable and unstable lowest mode are compared in Fig. 18. The distortions at the membrane center are what would be expected intuitively for unstable operation.

A 1.0 m model has been built and tested. This model has been used to obtain experimental information on the onset of instabilities. For a variety of membrane materials and rim mountings, the voltage on the membrane was increased until no further deflections were possible. The maximum achievable deflection was limited either by electrical discharge (corona or arcing) or by the onset of instabilities.

In one experiment the membrane was attached to the rim by springs. At quite modest deflections the membrane $z_e \simeq 0.6$ went unstable and quite slowly accelerated towards the back electrode as a unit. Visually the membrane behaved as if it had one degree of freedom and within the modest experimental accuracy the onset of instability occurred at the point predicted by a linear one-degree-of-freedom model, i.e., at an electrode membrane separation of two-thirds the initial separation.

For membranes attached rigidly to the rim, stable operation was possible with large deflections—with final membrane-electrode separations about 15% of the initial separation. As expected, this result is smaller than the prediction (40%) of one-degree-of-freedom cubic restoring force model.

Number of Electrodes

Associated with any mirror shape there is a pressure profile $p(r)$ required to exactly achieve the shape. This pressure profile directly determines the electric field required at the membrane surface since $p(r) = \epsilon_0 E^2(r)/2$ and this in turn determines the voltage profile required on the back electrode. The required profile for the 4.88 m diam $f_N = 3.5$ spherical mirror is shown as the smooth curve in Fig. 19. [To obtain this curve the voltage required was estimated as $E(r)$/(membrane-electrode separation).] This is a reasonable approximation if the voltage on the back electrodes varies slowly with position. In regions where the voltage varies rapidly, the electric field at the membrane surface is smoothed out over a distance comparable to the electrode membrane separation.

It is clearly impossible to exactly match the required back electrode voltage profile with a finite number of electrodes. The problem then is to determine the number of electrodes required to obtain a match close enough to provide a surface accurate to within the desired tolerances. It will be shown below that the stepped voltage profile (Fig. 19) obtained with five electrodes gives adequate surface quality with rms errors of the order of 15μm.

Although the voltage profile is discontinuous the pressure on the membrane will be a continuous funtion of r. (In practice there will be gaps between adjacent electrodes to avoid electrical breakdown. As long as the width of the gaps is small compared to the membrane electrode separation they do not significantly change the results.) The pressures on the membrane will have the desired profile at some point near the center of each electrode and also at radii near the gaps between electrodes. The pressure on the membrane will therefore oscillate around the desired profile with one cycle of oscillation for each electrode. In order to determine the effects of such pressure errors, the deflections produced by the pressure profile

$$p_n = p(r)\,[1 + \nu_n \sin(2n\pi r/R)] \tag{13}$$

was considered.

In order to determine the deflections produced by the pressure profile of Eq. (13), the full nonlinear equations for the membrane were solved to determine the pressure $p(r)$ required to give the desired spherical shape. The equations were then linearized about the solution to obtain the perturbations in the shape produced by the oscillating term. The resulting rms surface errors are then proportional to ν_n:

$$\sigma_n = \nu_n \Delta_n \tag{14}$$

and the values of Δ_n obtained from the numerical calculations are the circled points in Fig. 20. In order to check the reasonableness of the numerical estimates they were compared with the approximate estimate

$$\Delta_n \simeq d/12n^2 \tag{15}$$

where d is the unperturbed central deflection. (The estimate of Δ_n was obtained in the following manner. The linearized equations are second order so they are roughly comparable to $(d/dz)^2 y_n = \nu_n \sin nz$, which has the particular solution $y_n = -(\nu_n/n^2)\sin nz$. Therefore, one expects $\Delta_n = \alpha/n^2$. To obtain α note that for an initially untensioned membrane the central deflection d is approximately given by $kd^3 = p$ so that if $\delta p = \nu p$ then $\delta d = \nu d/3 = \alpha/n^2$. However, n is not well defined although intuitively a value between 0 and 1 seems appropriate. Arbitrarily setting $n = \frac{1}{2}$ gives the estimate of α and Eq. (15). This estimate is shown as the line in Fig. 20.

Considering the crudity and arbitrariness of the estimate, the agreement is astonishing.)

The voltage profile provided by five electrodes will match the desired pressure to within 5% so that the surface quality is roughly $0.05\Delta_5$ or about 15 μm.

The method of forming a mirror by electrostatically deflecting a membrane is ideally suited for surfaces whose radius of curvature varies slowly with positions. Deflections produced by a fluctuating pressure are smoothed out due to the elasticity of the membrane and the pressure on the membrane is a smoothed version of the voltage applied to the back electrodes. Conversely, the technique is ill adapted to the formation of surfaces with rapidly varying radii of curvature and should not be used for such applications.

Space Environment

Spacecraft have upon occasion suffered damage from electrical discharges caused by the interaction of the spacecraft with ambient plasmas. These difficulties, most severe at geosynchronous altitudes, are produced by the hot ($kT \simeq 10$-20 keV), low density ($n_e \simeq 1/\text{cm}^3$) plasmas encountered during geomagnetic substorms. In addition, at all altitudes there is an ever present cold plasma ($kT \lesssim 1$ eV, $n_e \simeq 10^2$-$10^4/\text{cm}^3$). The effect of this on ECMM performance must be considered.

Since the mirror surface is a conductor with a large radius of curvature electrical discharges due to differential charging will not be a problem.

During geomagnetic substorms the membrane will be bombarded by high energy (10-20 keV) electrons and protons and the membrane material must be able to withstand the effects of such a bombardment. In particular, electrons may penetrate the material, causing a charge build up and generating internal electric fields. The electric field strength is limited by the conduction of the charge back to the surface. The conductivity of the material increases as a consequence of the electron bombardment and at sufficiently high incident fluxes the amount of charge deposited is independent of the incident current. Studies[10] indicate that the saturation electric fields produced in Mylar will be substantially lower than breakdown even at the most severe space conditions.

The ECMM inherently involves large fields in the region between the mirror surface and the back electrodes. If the external environment has access to this high field region electrons and protons will be accelerated to high energies. The effects produced scale with plasma density and will be most severe at the high densities associated with a cold plasma. In order to avoid this situation, the working part of the ECMM must be encased in a Faraday cage which must not only provide electrical isolation but must prevent leakage of the plasma into the region between the electrodes and the mirror surface. This could be achieved, for example, with the material used for thermal isolation. Although some care must be taken, the space environment does not seem to pose any insurmountable obstacles to the ECMM.

Conclusion

The ECMM concept provides a unique method of obtaining high-gain reflectors with a mass significantly less than can be achieved by any other technique. The low mass is possible because the necessary stiffness of the reflector surface is obtained by tensioning a membrane with an electrostatically induced pressure loading. The high gain is obtained by adaptive closed-loop control using electrical forces to provide the necessary corrective pressure. The combination of high gain and low mass makes the ECMM ideally suited for space applications, and the space environment does not seem to impose any especially severe problems for the concept. A proposed ground-based 4.88-m-diam $f_N = 3.5$ reflector is described and the experimental and analytical basis for the design is given. It is found that five bullseye-shaped electrodes are sufficient to obtain a rms surface quality of 15 μm and that stable operation can be achieved with voltages in the 70 kV range.

Acknowledgments

This work was partially supported by Defense Advanced Research Projects Agency (DoD) under Contract DASG60-77-C-0123 and the Ballistic Missile Defense Advanced Technology Center, and NASA Langley Research Center, Contract NAS1-15548. Their support is gratefully acknowledged.

References

[1] Perkins, W.P. and Rohninger, G., U.S. Patent No. 4, 093,351, 1978.

[2] Jones, H.S., "Optical Scanning Using Electrically-Modulated Membrane Mirrors," IRCO Corp. Final Rept., ONR Contract Nonr-3649(00), 1962.

[3] Mrstik, A.V., Mihora, D.J., and Smith, P.G., *Spaceborne Millimeter-Wave Antenna Technology,* Vols. I and II, General Research Corp. CR-1-786, April 1978.

[4] "Submillimeter Wavelength Astronomy From Space," Rept. of the Submillimeter Space Telescope Working Group, Jet Propulsion Laboratory Rept. 740-3, April 1978.

[5] Mihora, D.J., Crawford, R.F., Redmond, P.J., and Cody, W.M., "Spaceborne Millimeter-Wave Antenna Technology, Vol. I—Membrane Reflector Technology," General Research Corp. CR-2-786, Aug. 1979.

[6] Mihora, D.J., Redmond, P.J., and Abbey, P.K., "Candidate Mirror Studies—Electrostatically Controlled Membrane Mirrors (ECMM): Phase II, Dynamics," General Research Corp., CR-2-740, Sept. 1977.

[7] Muller, British Patent No. 380,473, 1932.

[8] Jones, M.S., U.S. Patent No. 3, 522,483, 1967.

[9] Mihora, D.J., "Stresses in Adaptive Membrane Reflector," Presented at Eighth U.S. National Congress of Applied Mechanics, University of California at Los Angeles, June 1978.

[10] Beers, B.L., Hwang, H., Lin, D.L., and Pines, V.W., "Electron Transport Model of Dielectric Charging," NASA Conference Pub. 2071, AFGL-TR-79-0082, 1979.